THE ARCHIVES OF MECHANICAL ENGINEERING

VOL. LIII 2006 Number 1

Key words: *unsteady flows, MEMS wave engine*

JANUSZ R. PIECHNA *

NUMERICAL STUDY OF THE WAVE DISK MICRO-ENGINE OPERATION

Many groups of researchers have focused on the design of micro turbine engines in recent years. Since turbo-component efficiency becomes very low due to the downsizing effect, an important problem arises of how to obtain thermal efficiency high enough to produce the positive power required. The micro wave rotor is expected to be applied for the improvement of the performance of ultra micro gas turbines, increasing the cycle pressure ratio.

Wave rotors can also be built in another configuration. Applying only a combustion chamber and using oblique blades to form the rotor cells, net power can be taken from the rotor. In that way, the use in a micro scale of an inefficient turbo unit can be omitted. Such a solution in a form of wave engine was developed and practically realised by Weber [15] and Pearson [8], [9], [10] in centimetre scale. Conventional construction of wave engines in a form of wave rotor can not be directly realized in MEMS technology. The new idea of a wave disk developed by Piechna, Akbari, Iancu,and Mueller [11] and independently by Nagashima and Okamoto [7] gives the possibility of easy implementation of the wave engine idea in MEMS technology.

In the proposed solution, the wave disk plays the role of an active compression-decompression unit and torque generator. Appropriate port geometry with oblique blades forming the disk channels generates torque. The engine disk rotates with a speed much lower than the conventional turbo-unit that simplifies the bearing problem. Also, the construction of electric generator can be simpler.

The paper presents the proposed flow schemes, thermodynamic cycle, exemplary engine construction and some results of simulation of the MEMS wave engine using the wave disk.

1. Introduction

One can imagine a small, high performance, micro machines integrating an electrical motor or generator with steady or unsteady flow machinery for

* *Warsaw University of Technology, Institut of Aeronautics and Applied Mechanics; ul. Nowowiejska 24, 00-665 Warsaw, Poland; E-mail: jpie@meil.pw.edu.pl*

applications requiring compact power components, Epstein [1]. Specific ultra micro gas turbines made of stacked silicon wafer of millimetre scale, have low efficiency but a very high power to weight ratio. The energy density are 15 times and energy mass density 20 times higher than modern lithium batteries. In the future micro engines can be used as power sources for vehicles, communications equipment, mobile computers, robots and unmanned aircrafts. The ultra micro gas engine systems seem to be crucial for mobile technology for general use anywhere.

Estimated MEMS sales by technology area in the years 1998–2003 shows a higher than linear growth, mainly due to the unprecedented functionality they can offer.

Unfortunately, a dramatic lost of efficiency of conventional steady flow machinery (compressors and turbines) in small scale have been noticed. Even in millimetre scale, the conventional flow machinery requires values of tangential velocity equal to 400–500 m/s. Such high velocities in small scale causes a great viscous loses, Epstein [1], [3]. In conventional turbo-machinery systems, great part of the power generated by the turbines had to be reversed (returned) to compressor. Only small part of power cycling in turbine – compressor system is the net power. Taking into account low efficiency of the turbine-compressor team, the total efficiency of the engine is low. Wave rotors can be used as topping unit increasing the total compression ratio and due to the self cooling mechanism increasing the working gas top cycle temperature.

Wave rotors can also be used in another configuration. Applying only a combustion chamber instead of a supercharged engine, and using oblique ports with vanes and oblique blades to form the cells, net power can be taken from the rotor. Appropriate port geometry with oblique rotor blades forming rotor channels generates torque.

In the mid 1950s, Pearson [8], [9], [10] designed a unique wave rotor known as the wave engine. The relatively very short rotor had helical channels which changed the direction of gas flow, generating shaft work. The engine worked several hundred hours in a wide range of operating conditions showing, at low rotational speed, higher efficiency than a comparable conventional turbo engine. The engine had a complicated porting system for realisation of multi-stage gas compression and decompression. One of engine version operating in the range of 3 000 to 18 000 rpm, produced up to 26 kW at its design point, with peak temperature of 1070 K and thermal efficiency of about 10%. It is known as the most successful wave rotor machine built to date. Similar wave engine was proposed by Weber [15].

Analogue solutions can be used in MEMS technology. However, it can not be done in a direct way. The geometry of conventional wave rotors is

not suitable for the MEMS technology. Only wave discs with flat geometry can be applied in silicon wafer technology. In the present work, the author has proposed a solution on the basis of the wave disc geometrical configuration with porting system realising two stage compression-decompression processes to increase the total efficiency. Middle pressure by-pass was used additionally for generating the torque and consequently net power.

Assuming the outer radius of the wave disc equal to 15 mm, inner disc radius of 6 mm and height of the disc of 1 mm with doubled set of ports, the operational rotational speed is assumed to be equal to 160 000 rpm. It is 2 times lower than that used by the conventional turbo-machinery.

According to Epstein [2], [3] and Frechette [5], [6], the motor-generator can be integrated within the engine. Such a solution offers the advantages of mechanical simplicity. In the proposed construction, it is assumed that the rotating wave disc has imprinted elements of the rotor electric circuit. The multi-pole planar electric induction machine can be mounted on the shroud of the wave disc. Switching and control circuitry can be design as an external part.

MEMS technology offers the capacity to fabricate static and dynamic axial and journal bearing as well as induction motors-generators, which can be used for disc speed control. Due to their flatness and radial symmetry, wave discs can easily be adapted to micro gas engine constructions.

Bearing system, stabilizing radially and axially conventional turbine-compressor unit, had to work in extreme conditions: high rotational speeds and high temperatures. Existing up to date bearing constructions can work at high rotational speeds but not at so high temperatures. Low rotational speeds, required in the presented construction, also lowers the problem of electric generator and frequency converters.

This paper presents an application of new ideas in MEMS wave engine design. The idea of wave discs is relatively young, and is not commonly known [4], [11], [12]. There aren't any known solutions of wave engines in radial geometry. Probably up to now, radial wave rotors have been omitted because of negative influence of centrifugal forces on the compression process. Papers [11], [12] shows methods suitable for the control of these forces. New trends in developments of small turbo-engines, having a low efficiency due to the scaling effect, generated the need of devices increasing efficiency (like recuperators). One of such ideas is the application of the wave rotor as a turbine topping unit. The main problem of conventional constructions of the wave rotors in such applications are bad scavenging properties. However, the compression process is realised without special problems, although purifying the wave rotor cells is problematic when the back-pressure is too high. The proposed solution in a form of radial rotor having curved channels can over-

come this problem adding, in a controllable way, an additional force (being the component of centrifugal forces) improving the scavenging process. Idea of wave disk engine has one shortcoming – the low compression ratio reducing the total efficiency. Some other solutions using pre-compression had to be considered. In the proposed engine construction, a two stage compression-decompression scheme in radial configuration was applied. The analysed system is strongly nonlinear and difficult to simulate. This paper presents preliminary results of numerical simulation of the wave engine operation in micro-scale. New and unknown physical phenomena accompanying compression and expansion processes in curved channels of radial rotors have been shown. It might be possible that wave discs can solve of the micro-engine problem of very low efficiency.

2. Physical model

Thermodynamic cycles of the conventional turbo-engine and wave-engine are shown and compared in Fig. 1. In the presented drawing the compression and decompression process efficiency in turbo-compressor and wave-compressor were assumed to be the same. In the micro scale, efficiency of wave compression is higher.

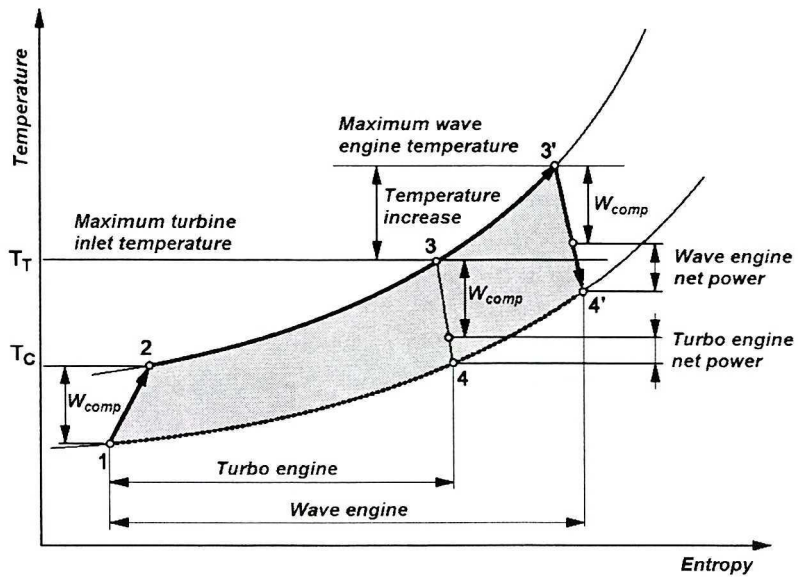

Fig. 1. Schematic Temperature-Entropy diagram for turbo-engine and wave-engine

A schematic thermodynamic cycle is presented in Fig. 1. The turbo-engine cycle is represented by points 1-2-3-4, and the wave-engine cycle

is represented by points 1-2-3'-4'. Line 1-2 represents compression by the compressor or unsteady flow in wave engine, lines 2-3 and 2-3' describe heat delivery in the combustion chamber, lines 3-4 represent power generated by the turbine, line 3'-4' shows the hot gases expansion in wave engine, lines 4-1 and 4'-1 describe heat release into the atmosphere.

At the same compression pressure ratio, the increase of top wave-engine cycle temperature is evident. Due to the self cooling phenomena characteristic to the wave processes, the top cycle temperature in the wave-engine can by higher than in the turbo-engine.

Air compression power W_{comp} must be compensated by the part of the turbine power or hot gas expansion power. In the turbo-engine, the compression power must be transferred by the shaft from the turbine. The wave engine exchanges compression energy directly between hot exhaust gases and fresh cold air, and due to that only the net power has to be extracted from the flow. The net turbo-engine power and net wave-engine power are shown on the scheme.

The simplest flow scheme of a wave engine is basing on the wave diagram shown in Fig. 2. On the left side of the drawing, schematic wave diagram with position of all ports is presented with corresponding state plane on the right side. Flow parameters in the areas on the wave diagram separated by waves, compression and expansion, are constant and are described by the corresponding points on the state plane. Numbers in wave diagram areas have equivalents on the state plane.

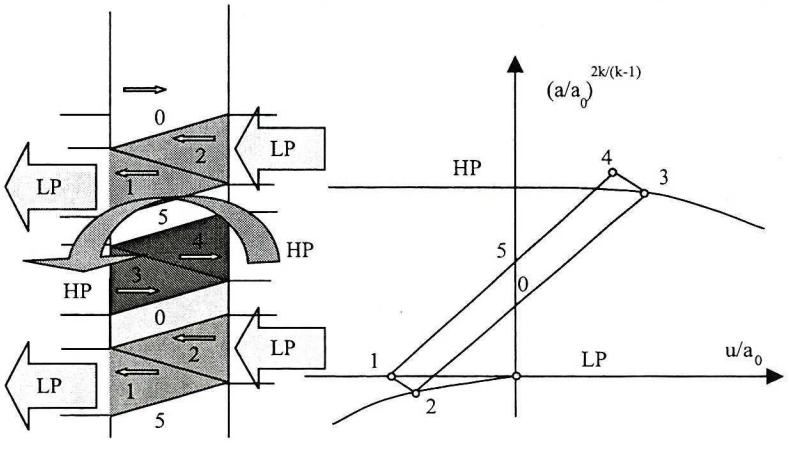

Fig. 2. Wave-engine wave diagram and corresponding state plane

Expanded exhaust gases are rejected to the atmosphere (area 1) generating expansion wave inducing inflow of the fresh air (area 2). Fresh air is compressed (are 3) by the high pressure hot gas from combustion chamber.

Compressed air (area 4) is delivered to the combustion chamber. After heating in combustion chamber, the hot mixture of air and exhaust gases is used for fresh air compression and after expansion is rejected to the atmosphere.

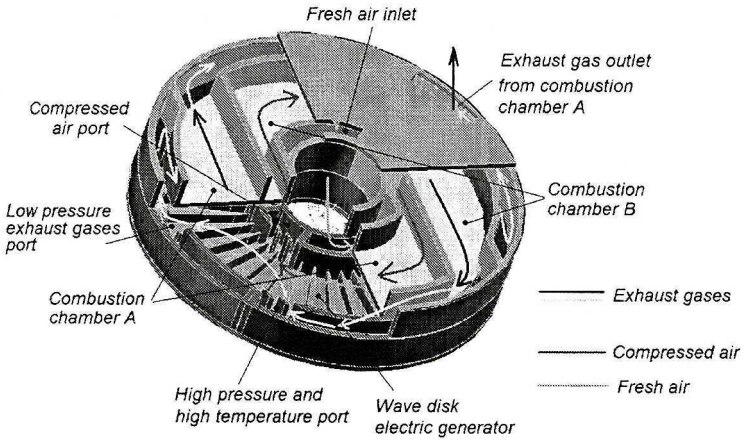

Fig. 3. Details of the wave engine construction

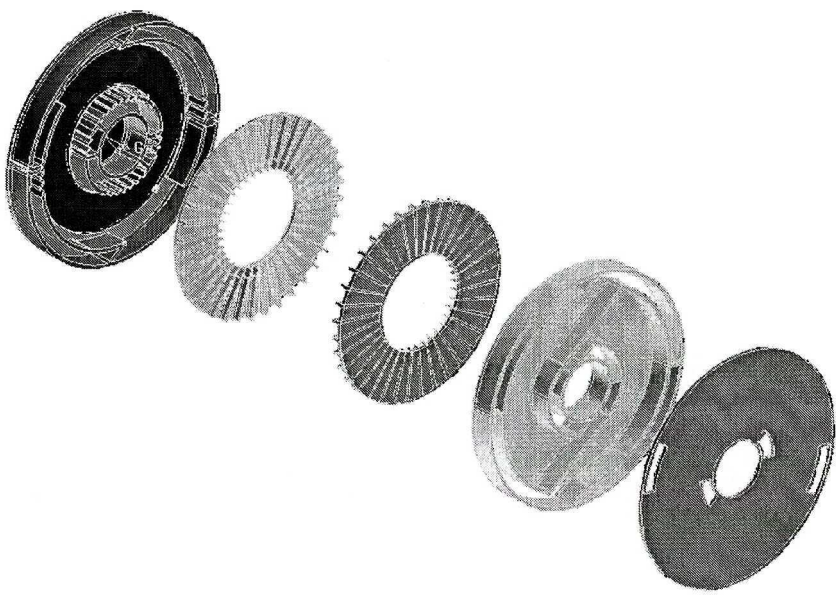

Fig. 4. Exploded view of the wave-engine construction

An exemplary construction of micro-engine in MEMS technology was visualized in Fig. 3. In the presented construction, a double port set with two

parallel operating combustion chambers was applied. Arrows in the figure explain the used flow field scheme.

An exploded view of main wave-engine components is shown in Fig. 4. The engine case can be prepared as a three part set. The most complicated part contains the basic plate with all port arrangements. The second part forms the combustion chambers and outflow mufflers. The third part is only the cover with air inlets and exhaust gases outlets. Wave disk can be formed as two parts etched together.

The electric motor-generator can be imprinted in the case part containing ports and in one of parts forming a wave disk, as it is shown in Fig. 5.

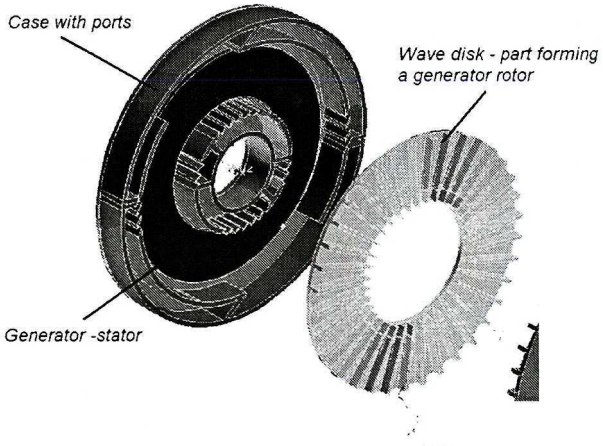

Fig. 5. Hypothetic electric motor-generator arrangement

The scheme of the flow through the combustion chambers is schematically presented in Fig. 6.

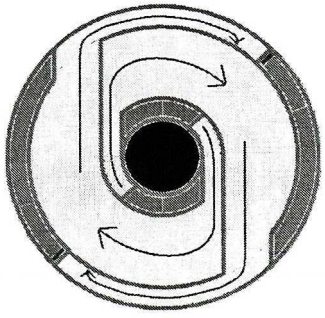

Fig. 6. Schematic flow arrangement inside both combustion chambers

Analysing details of construction of the only one successful wave engine realisation [8], [9], [10], developed by Pearson, one can easily notice two-stage compression and decompression process applied in this engine. However, any data about pressures, velocities and flow rates are not available, although there is no doubt that the success of construction lays in a two-stage compression principle.

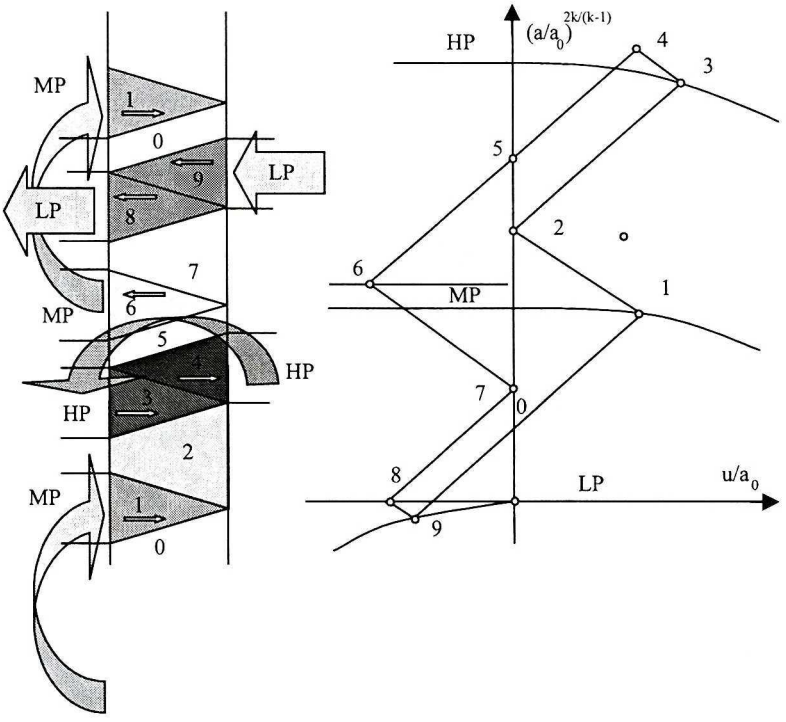

Fig. 7. Two step compression micro-engine wave diagram and corresponding state plane

In the proposed micro-engine construction two-step gas compression-decompression idea was adopted. The micro-engine proposed porting scheme, simplified wave diagram and state plane are presented in Fig. 7. In the proposed solution, two middle pressure gas ports (inlet (port A) and outlet (port C)) connected by passage, and low pressure gas outflow port (port D) the high pressure gas port (port B) are located at the outer side of the wave disk. The high pressure air port (port E) and low pressure fresh air port (port F) are located at the inner side of the wave disk. In such a configuration, the fresh air enters the cell with pressure and velocity described by the position of point 9 on state diagram, then air is compressed to state 1 on the state plane by the middle pressure gas entering the cell from the middle pressure passage with parameters described by point 6, and air finally is compressed to the state 4 by the high pressure gas. The air, compressed two times to the

high pressure, is delivered to the combustion chamber. After mixing with the fuel, it forms the mixture burned inside the combustion chamber. Hot, high pressure gases leave the combustion chamber and enter the cell at state 3 realising the second step of air compression. Then, exhaust gases leave the cell and through the medium pressure passage (state 6) enter the wave disc cells again (state 1) realising the first stage of air compression. Exhaust gases finally, after decompression, leave the cell to the exhaust port (state 8). The port's geometry and flow diagram are developed in such a way that the hot gases are concentrated near the outer part of the wave disk and cold air concentrates near the inner disk part. On the one hand, such configuration generates the disk nonuniform temperature distribution and thermal stresses, but on the other hand reduces the heat exchange between disk walls and cold air and hot gas. Generally, this flow arrangement can be classified as the reversed flow configuration. The proposed flow scheme is different from that used by Pearson [8]. The flow scheme was matched to the radial wave rotor geometry used in the proposed solution. It was assumed that centrifugal forces can improve the flow during the scavenging and slightly disturb the compression process. During the compression process, there exists enough energy to overcome negative influence of centrifugal forces. During the end of scavenging process, there always exists a lack of energy to completely remove exhaust gases from cells. Centrifugal forces act in a way improving the scavenging process in the proposed configuration.

3. Mathematical model

Flow scheme in the analysed engine configuration is rather complicated, and flow rates strongly conjunct. The mass flow rate in the compressed air (high pressure) port (port E) should be equal (omitting 3% of fuel mass added) to the mass flow rate at high pressure of hot gas port (port B). Simultaneously, the mass flow rate in middle pressure level ports (ports A and C), connected by passage, have to be the same. The flow is additionally affected by the action of centrifugal forces dependent on the actual rotational speed and the local radius. Prediction of proper port timing for engine in such a configuration is very difficult. The amount of energy generated in the combustion chamber and transferred to the working fluid has a crucial influence on the wave engine operation. There are sophisticated codes used for two and three dimensional calculation of unsteady processes in engine system under consideration exist. However, they can not be used for port geometry prediction. Because of that, a specialised program based on the one-dimensional approximation was developed and used for finding the proper port timing.

4. Governing equations

In the proposed engine disk configuration, the cells are located in one plane perpendicular to the axis of the disc rotation, generally in radial direction. The cell shape can be strait, or can be more complicated, forming a curved channel with variable cross-section. Due to generally radial cell location, the influence of the centrifugal forces acting on the gas mowing inside the cell had to be taken into account. One of possible cell shapes is shown in Fig. 8.

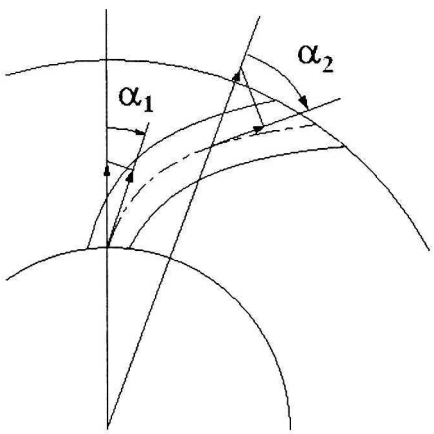

Fig. 8. General shape of the single wave disk's cell

To prepare the mathematical model of the micro-engine operation, it was assumed that the flow in each cell is unsteady and the fluid is a compressible, ideal gas. In the analysis presented, the following assumptions and simplifications were used: because the perfect gas constant R equals 287 for air, and about 290 for the exhaust gas, and the value of specific heat ratio equals 1.4 for air and 1.38 for the exhaust gas, it was assumed that only one gas, having air parameters (R = 287 and k = 1.4), would be used for simulation of micro-engine operation. The flow is treated as non-adiabatic with possible heat exchange by cell walls. The viscosity of the fluid is represented only by a wall friction coefficient. The cell cross-section can be varied along the cell length. The existence of centrifugal mass forces is included in the momentum equation.

Under the assumption presented above, an unsteady flow of gas in a single cell can be described by the following set of equations, which are a modified version of one-dimensional Euler equations (Shapiro [13]) written in conservative form:

$$\frac{\partial U}{\partial t} + \frac{\partial F}{\partial x} + B = 0$$

with

$$U = \begin{pmatrix} \rho \\ \rho u \\ \rho e \end{pmatrix}; \; F = \begin{pmatrix} \rho u \\ \rho u^2 + p \\ u(\rho e + p) \end{pmatrix}; \; B = \begin{pmatrix} \rho u \dfrac{dA}{Ads} \pm \dfrac{\dot{\bar{m}}}{A} \\ \rho u^2 \dfrac{dA}{Ads} + \rho f \dfrac{u|u|}{2} \dfrac{1}{D} - \rho \omega^2 r \cos\alpha \pm u \dfrac{\dot{\bar{m}}}{A} \\ u(\rho e + p) \dfrac{dA}{Ads} - \dfrac{q}{A} \pm e \dfrac{\dot{\bar{m}}}{A} \end{pmatrix};$$

$e = \dfrac{u^2}{2} + \dfrac{1}{k-1} \dfrac{p}{\rho}$; (3.2) where:

term $\dfrac{dA}{Ads}$ represents variation of the cell cross-section along the cell,

$\dot{\bar{m}}$ – is a mass flow rate representing the leaks between the rotor and case,

q – is a heat flux exchanged by the cell walls,

f – is the friction factor,

A – is a local cell cross-section area

r – local distance to the axis of rotation

ω – angular speed of rotation

$\dot{\bar{m}}$ – local leakage

α – local angle between radius and cell axis.

However, the Euler equations describe the unsteady flow of compressible fluid in the rotor cells, and formation of the wave structure inside the cell is caused by the specific boundary conditions.

In the described micro-engine model, each cell's end is periodically connected to large vessels containing gas of pressure and temperature changing in time.

5. Boundary conditions

In many papers describing PWE operation the authors concentrate their attention only on the governing equations and the numerical method of solution used, omitting the problem of boundary conditions. In the analysed case one can deduce the existence of a few typical flows patterns. Generally, it is the inflow from the pressure vessel to the cell. Gas parameters in the vessel and cell can be different, which means that the entropy (temperature and density) discontinuity surface will arrive (see Fig. 9). In some phases of the device's operation an outflow from the cell to the vessel will be expected. It is necessary to consider the possibility of choked flow conditions (case of

$M_1 = 1$ in Fig. 9). Periods of operation when the cell ends are closed also exist.

In the proposed model, the following boundary conditions have been applied.

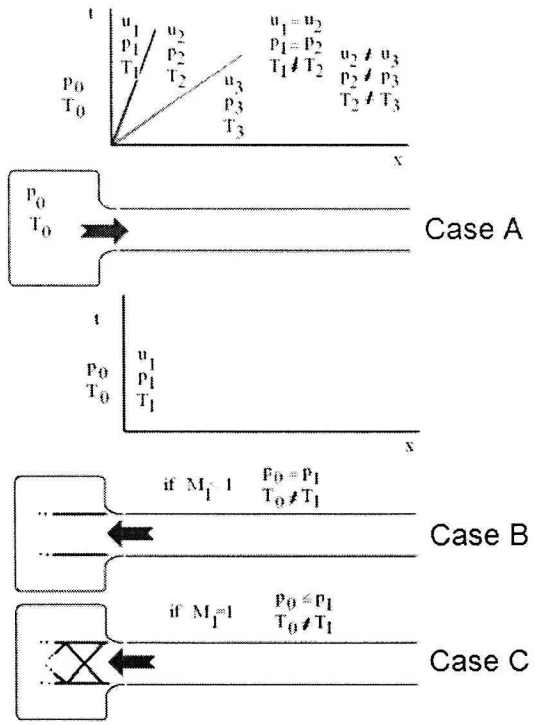

Fig. 9. Scheme of the left boundary condition

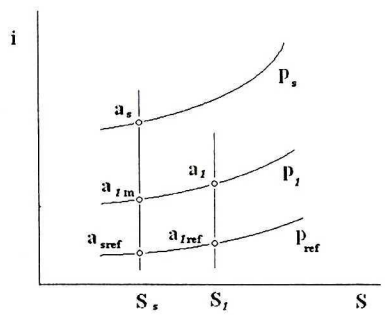

Fig. 10. Enthalpy-entropy diagram showing the conditions on both sides of the discontinuity surface

It was assumed that cells open immediately to the appropriate vessel and that the stagnation values of gas pressure and gas temperature in vessels are known.

An enthalpy-entropy diagram explaining possibility of temperature discontinuity existence during initial stage of gas inflow to the cell is shown in Fig. 10. Using the same reference pressure p_{ref}, differences in entropy levels on both sides of the discontinuity with the same pressure p_1, we can represent by the ratio of the speeds of sound a_{1m} and a_1.

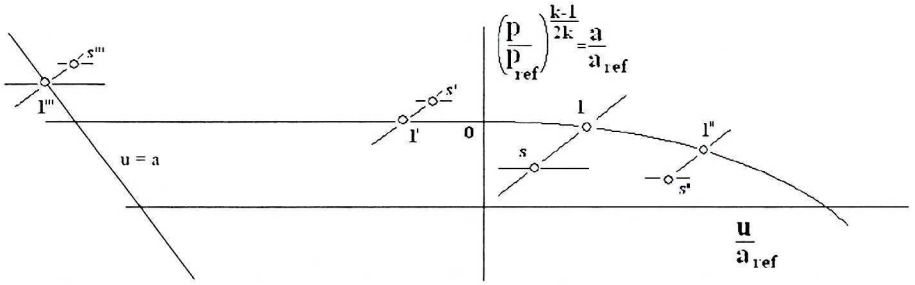

Fig. 11. State plane describing possible solutions to left boundary conditions (typical inflow to the cell s''-1'', typical outflow from cell s'-1', chocked outflow s'''-1''')

A state diagram for the left boundary condition is presented in Fig. 10. A solution to the boundary conditions is obtained assuming the existence of locally isentropic, quasi-steady flow between the vessel and the inlet cell cross-section, and then assuming unsteady flow in the cell. Steady flow conditions are described by the energy equation. The unsteady relation in the cell is defined by the compatibility equation on the bi-characteristic of family II (Shapiro [13]).

The boundary condition of the single cell unsteady flow process is solved assuming that the cell end volume connection is rapid. Due to the relatively short time of the opening and closing processes in comparison with the unsteady flow processes in the cell, such simplification seems to be justified.

The schematic geometry of the cell – volume connection and possible general flow parameters on the physical plane (x-t) are presented in Fig. 9.

Depending on the temporary pressure and velocity values inside the cell, three basic cases must be considered:

Case A – a subsonic inflow from the volume to the cell (sometimes behind the shock wave),

Case B – a subsonic outflow from the cell to the volume (M1 < 1 see Fig. 9),

Case C – a sonic outflow from the cell to the volume (M1 = 1 see Fig. 9).

While the solution of Euler equations inside the cell is obtained by the Lax-Wendroff scheme, only the primitive variables (ρ, u, p) are stored at each node.

6. Port parameters

The engine is connected with the atmosphere through the fresh air inlet port (port F on the inner side of the wave disk) and the exhaust gas outlet (port D on the outer side of the wave disk). In these ports, flow parameters are well defined by the atmospheric pressure and ambient temperature. The rest of ports are the internal connection ports, and pressure and temperature are defined by the inflow and outflow parameters.

6.1. Combustion chamber

The compressed air leaving the wave disk through port E, located on the inner disk side, is delivered to the combustion chamber, then heated and returned to the cells of the wave disk through the port B on the outer side of the disk. Pressure and temperature in the combustion chamber can be calculated from the energy and continuity equation and the equation of state.

$$\frac{dp}{dt} = \frac{k-1}{V_{comb}}\left(\rho_{air}u_{air}F_{air}\left(\frac{kRT_{air}}{k-1} + \frac{u_{air}^2}{2} + \frac{V_{out}^2}{2}\right) - \rho_{gas}u_{gas}F_{gas}\left(\frac{kRT_{gas}}{k-1} + \frac{u_{gas}^2}{2}\right) + Q_{comb}\right)$$

$$\frac{dm_{Vcomb}}{dt} = \rho_{air}u_{air}F_{air} - \rho_{gas}u_{gas}F_{gas}$$

$$T = \frac{pV_{comb}}{Rm_{Vcomb}}$$

6.2. Medium pressure passage

In the proposed construction of micro-engine, a two-step air compression and exhaust gas decompression is introduced. The medium pressure passage is used to decompress the exhaust gases from the high pressure to the medium pressure and use it to realisation of the first step of air compression. Pressure and temperature in the medium pressure passage are a result of equilibrium of the exhaust leaving the wave disk at port C, on the outer disk side, and entering the wave disk through the port A, also on the outer disk side. The exhaust gas parameters in the passage can be calculated in a similar way to that used for combustion chamber.

$$\frac{dp}{dt} = \frac{k-1}{V_{pass}}\left(\rho_{out}u_{out}F_{out}\left(\frac{kRT_{out}}{k-1} + \frac{u_{out}^2}{2} + \frac{V_{out}^2}{2}\right) - \rho_{in}u_{in}F_{in}\left(\frac{kRT_{in}}{k-1} + \frac{u_{in}^2}{2}\right)\right)$$

$$\frac{dm_{pass}}{dt} = \rho_{out}u_{out}F_{out} - \rho_{in}u_{in}F_{in}$$

$$T = \frac{pV_{pass}}{Rm_{pass}}$$

7. Torque calculation

The flow scheme in the analysed micro-engine was designed to generate a net power. In the actually proposed engine version, only a straight cells are used. All ports in which the flow is in disc direction is expected are assumed to be equipped with vanes directing the port flow almost tangentially to the disc. The torque can be calculated from equation of continuity and spin conservation. Only in relatively narrow range of engine port geometry and rotational speed, the positive torque and power can be generated.

8. Results of simulation

The numerical code written in Fortran on the basis of the presented mathematical model has been developed and used for simulation of the micro-engine operation. Due to strongly nonlinear system of equation solved, the code was developed in a way offering the user an easy way of changing geometrical and technical parameters of the analysed micro-engine. Several simulations have been performed for predefining a proper micro-engine geometry, rotational speed and heat released in the combustion chamber for a stable wave engine operation.

Each simulation starts from initial conditions assuming all pressures equal atmospheric pressure and zero velocity. Only disk rotational speed and heat release in the combustion chamber are defined and kept constant. All pressures, velocities and temperature distributions are build up and formed in a transient process. After 160 cycles of operation, steady state engine operation conditions are achieved.

The following set of figures depicts a set of basic information about the engine operation. In each figure on the left side a conventional wave diagram with position of all ports is shown. X – axis corresponds to the position along the cell in radial direction, while y-axis represents angle position or time. Although the engine has a double set of ports, only single set corresponding to single period of device operation is presented here. The left side of this

diagram corresponds to the outer side of the wave disc and the right side to the inner side of the disc. In this diagram, velocity variation in time on both cell ends are presented in each figure.

A real radial disc configuration with double set of ports is presented in the right side of each figure. The wave disk is rotating in clock-wise direction. Path lines are additionally visualised in each figure.

Exemplary pressure distribution inside the single step compression wave-engine is presented in Fig. 12. Corresponding temperature distribution is shown in Fig. 13.

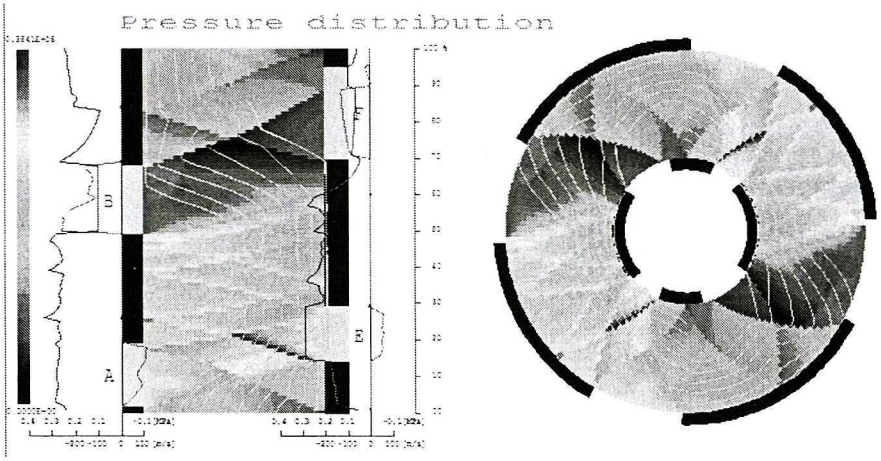

Fig. 12. Pressure distribution inside the wave disc of single step compression wave engine

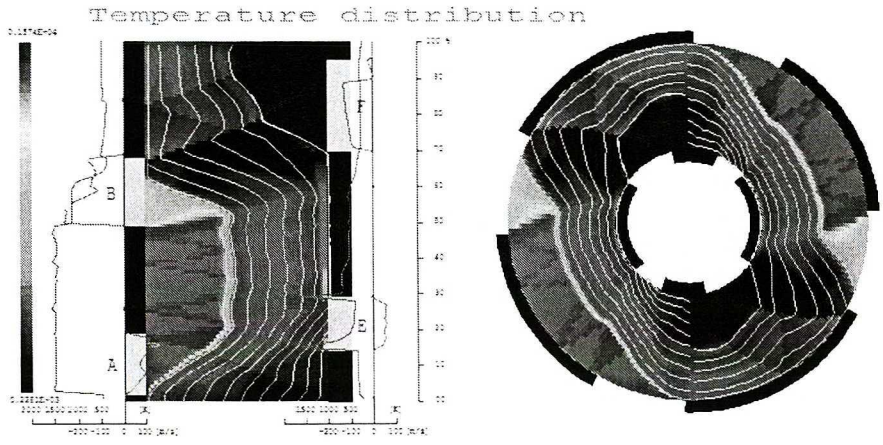

Fig. 13. Temperature distribution inside the wave disc of single step compression wave engine

All results presented in Fig. 12 and Fig. 13 correspond to the case of heat release stream equal to 800 W and disc rotational speed equal to 200 000 rpm.

In the case of single compression step, the wave engine estimated efficiency was about 6%.

More attention was concentrated on the two-step compression version of the wave-engine. All results presented below correspond to the case of heat release stream equal to 800 W and disc rotational speed equal to 176 500 rpm.

It have been found by the simulation, that there exists a relatively narrow range of parameters, in which the engine works stable.

Pressure distribution inside the wave disk strait cells is presented in Fig. 14.

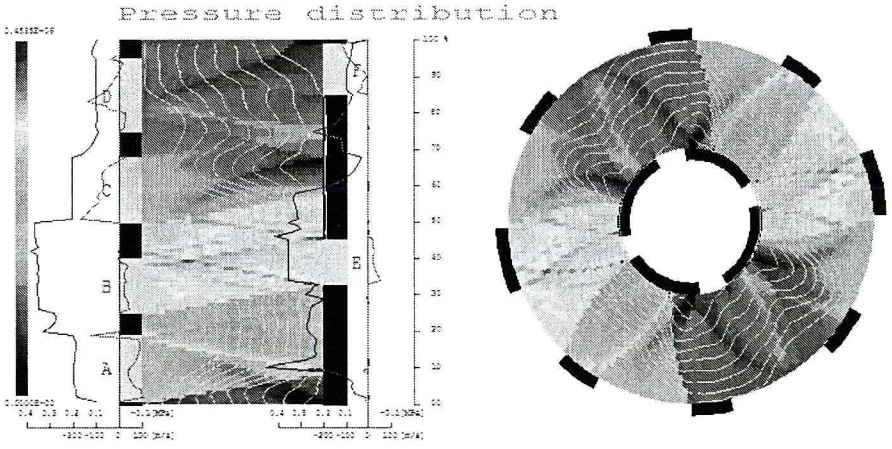

Fig. 14. Pressure distribution inside the wave disc of the two step compression wave engine

Althouht, the engine is operating generating net power, one can notice that some port geometry can be optimised, for example, to omit reverse flows in port A and D. Wave propagation can be easily recognised and tracked. One can notice a lot of reflection and additional waves generated at almost all port edges. Three basic pressure levels, expected in the considered configuration, are clearly visible. As expected, the highest pressure level is observed near port B (high pressure exhaust gases port) and port E (high pressure compressed air port) representing the second and final compression step. Medium pressure is observed near port C (partial expansion of exhaust gases port) and near port A (first step of air compression). From the path line shape, the first step of the air compression can be easily identified in vicinity of port A. The compression process is confirmed by the pressure level on the right closed side of the cell. Two steps of exhaust gas decompression can be also identified.

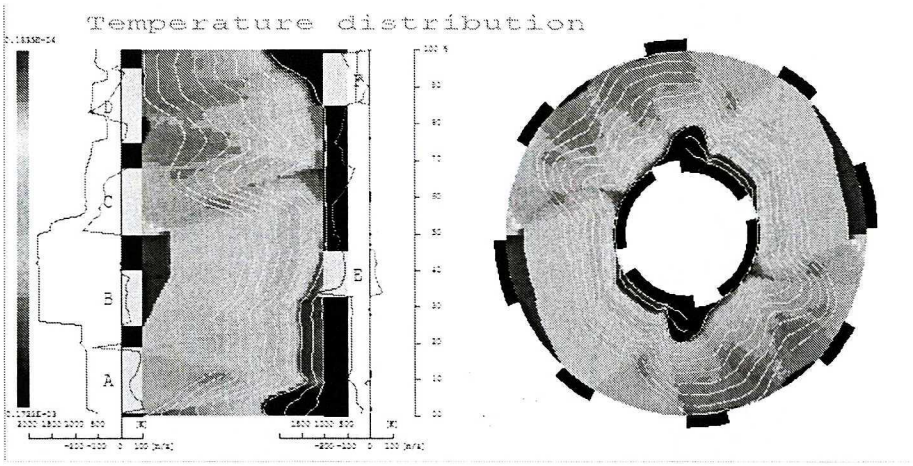

Fig. 15. Temperature distribution inside the wave disc of the two step compression wave engine

Temperature distribution inside the wave disc is shown in Fig. 15. The only characteristic feature is limited and well defined area of the highest temperatures. After partial decompression to the medium pressure level, the temperature of the exhaust gases is significantly reduced. Cold fresh air is efficiently separated from the hot exhaust gases by the layer of the medium pressure warm gases. The compressed air has relatively very low temperature when it is delivered to the combustion chamber.

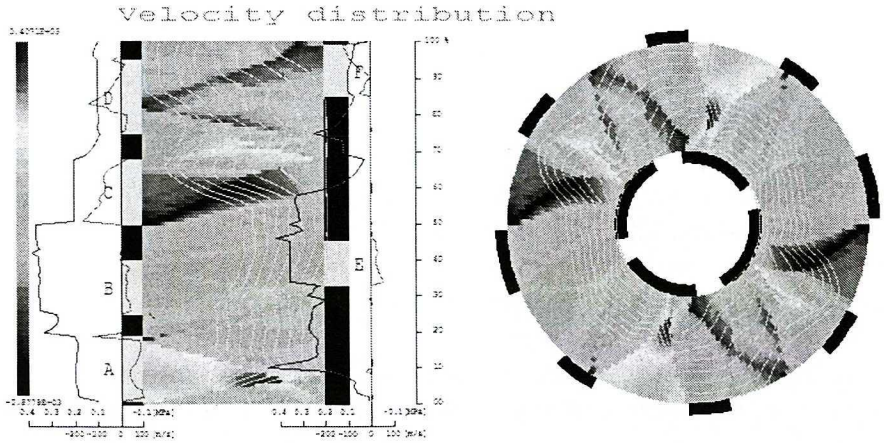

Fig. 16. Velocity distribution inside the wave disc of the two step compression wave engine

Velocity distribution inside the wave disc is depicted in Figure 16. The strong inflow to the wave disk from port A and outflow through port C is evident. Path line shapes suggest that the scavenging process is intensive. All the amount of exhaust gases is ejected to the atmosphere.

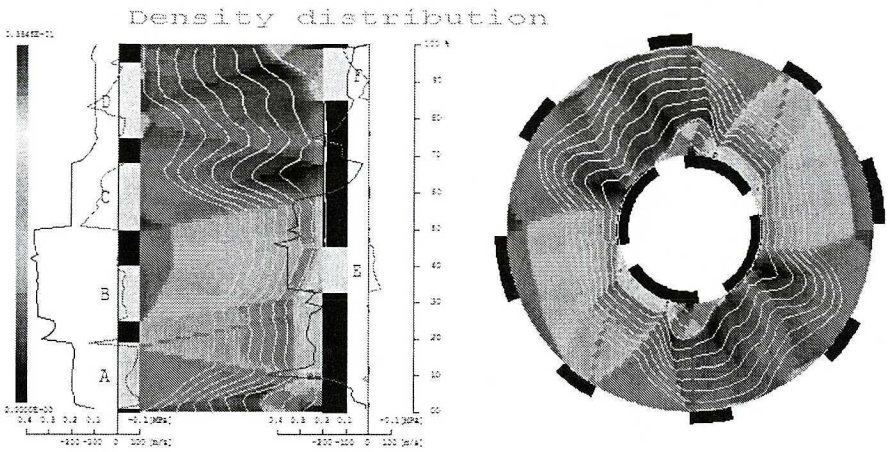

Fig. 17. Density distribution inside the wave disc of the two step compression wave engine

Density distribution in the wave disc is shown in Fig. 17. Low density values can be observed in high pressure exhaust gases area. One can notice the increase of the compressed fresh air density after the first compression step. Correlating path lines with the density change, one can easily recognise the first and the second compression process finished by the compressed air delivery to the combustion chamber.

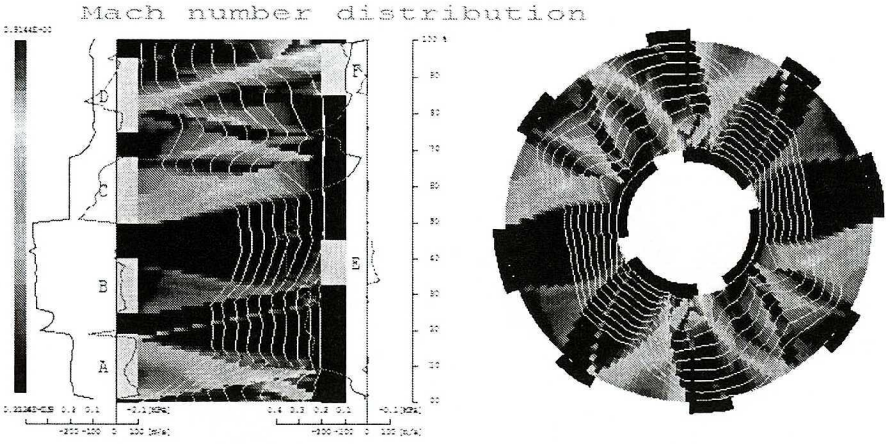

Fig. 18. Mach number distribution inside the wave disc of the two step compression wave engine

Distribution of the Mach number presented in Fig. 18 provides some additional information. Due to the variable cell geometry (cell cross-section increases while coming to the outer side of the disc) the Mach number is reaching transonic regime. This is rather unexpected phenomenon and it can cause problems.

Many simulations that have been performed show, in the analysed port geometry, a rather very narrow range of rotational speeds and accepted heat streams. Outside the operational regime, one observes very oscillatory and unsteady flows.

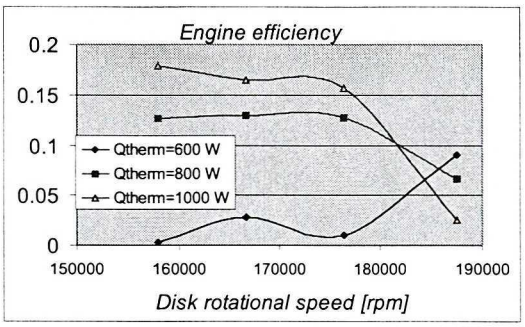

Fig. 19. Engine efficiency in function of disk rotational speed and combustion chamber heat release (two step compression wave engine)

The predicted micro-engine efficiency, in stable operational area is presented in Fig. 19. The presented results show potential strength of the proposed micro-engine construction. Actual micro-engine geometry is not optimal and needs a comprehensive investigation.

Although, the presented port geometry is not the final one, we have proposed a construction of the two step compression engine in MEMS technology (Fig. 20).

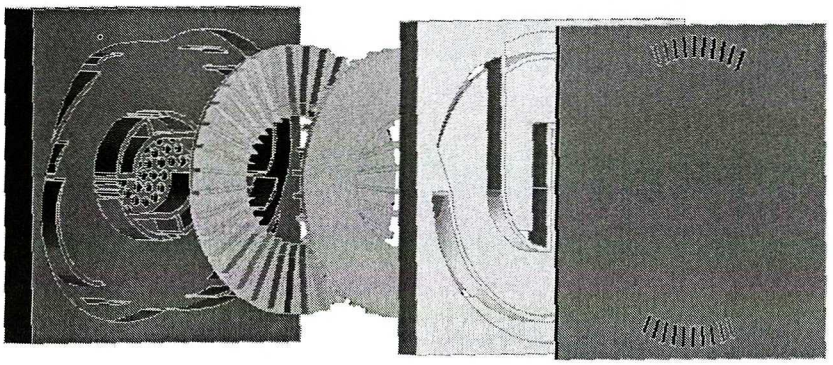

Fig. 20. Exploded view of the main components of the two step compression wave-engine

The proposed channels and ports geometry is depicted in Fig. 21.

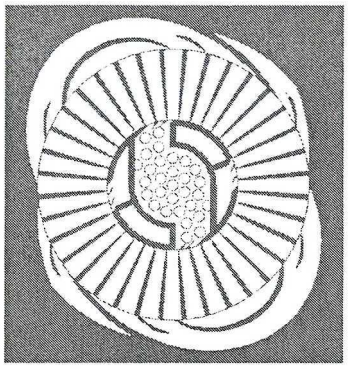

Fig. 21. Proposed channels and port set geometry of the two step compression wave-engine

Taking into account the results of simulation, one can define the engine starting procedure. During the start procedure, engine generator operates in the starter mode increasing the disk rotational speed to the operational range using the electric energy from a battery. After the operational disk speed is reached, fuel is delivered to the combustion chamber and burned. The engine generator is then switched to the generator-controller mode delivering electric energy to the battery and controlling the actual operational disk rotational speed. Due to relatively narrow range of operational parameters (heat delivery and rotational speed), it is very important to developed very sophisticated control system regulating the amount of fuel delivered and load of the electric generator to keep the disk rotational speed in the operational range.

9. Conclusions

The paper presents a concept of micro-engine construction utilizing the unsteady phenomena to reach the micro-engine efficiency higher then that in conventional steady state flow machinery. The proposed idea is confirmed by the numerical simulation showing the potential range of operational parameters and predicted engine efficiency. It should be noticed that the really working wave engine developed and build by Pearson [8], [9], [10] had the efficiency of about 10% in the operational point. Although the applied mathematical micro-engine model does not take into account all physical phenomena (heat transfer from the gas to disk walls is neglected, leakage in the disk case gap is omitted, gradual cell opening process is not taken into account) the obtained numerical simulation results suggest that the micro-engine of the proposed construction can deliver a net power in micro-scale with reasonable efficiency. The presented work concentrated on considering

the unsteady flow phenomena omitted the problem of bearing construction, heat transfer problems and construction thermal stresses. It seems that this work can be a good basis for building more sophisticated 2-D and 3-D models using commercial codes like Fluent.

Manuscript received by Editorial Board, July 28, 2005

REFERENCES

[1] Epstein et al, 1997, Micro-Heat Engines, Gas Turbines, and Rocket Engines-the MIT Micro-engine Project, Paper 97-1773, AIAA Fluid Dynamics Conference, Snowmass Village.

[2] Epstein A. H., Jacobson S. A., Protz J. M., Frechette L. G.: 2000, Shirtbutton-Sized Gas Turbines: the Engineering Challenges of Micro High Speed Rotating Machinerry, Proc of 8tj Int. Symp. On Transp. Phenom. And Dyn. Of Rot. Machinery (ISROMAC'8), Honolulu, Hawaii.

[3] Epstain A. H.: 2003, Millimeter-scale, MEMS gas turbine engines, GT-2003-38866,Proc of ASME Turbo Expo 2003, June 16–19, 2003, Atlanta, Georgia, USA.

[4] Frąckowiak M., Iancu F., Potrzebowski A., Akbari P., Müller N., Piechna J.: 2004, Numerical simulation of unsteady flow processes in wave rotors, IMECE2004-60973.

[5] Frechette L. G.: 2000, Development of a Microfabricated Silicon Motor-Driven Compression System, PhD at MIT.

[6] Frechette L. G.: 2001, Assessment of Viscous Flows in High-Speed Micro Rotating Machinery for Energy Conversion Applications, IMECE'01/DAC-1234.

[7] Nagashima T., Okamoto K.: 2005, Experimental investigation of the wave discs. Private communication.

[8] Pearson R. D.: 1982, "Pressure Exchangers and Pressure Exchange Engines," Chapter 16, The Thermodynamics and Gas Dynamics of Internal Combustion Engines, Vol. 1, Benson, R., Oxford University Press., pp. 903÷940.

[9] Pearson R. D.: 1983, "A Pressure Exchange Engine for Burning Pyroil as the End User in a Cheap Power from Biomass System", 15th International Congress of Combustion Engines, Paris.

[10] Pearson R. D.: 1985, "A Gas Wave-Turbine Engine Which Developed 35 HP and Performed Over a 6:1 Speed Range, " Proc. ONR/NAVAIR Wave Rotor Research and Technology Workshop, Report NPS-67-85-008, pp. 403÷49, Naval Postgraduate School, Monterey, CA.

[11] Piechna J., Akbari P., Iancu F., and Müller N.: 2004, Radial-flow wave rotor concepts, unconventional designs and applications, IMECE2004-59022.

[12] Piechna J.: 2005, "Wave Machines, Models and Numerical Simulation", Oficyna Wydawnicza Politechniki Warszawskiej, Warszawa.

[13] Shapiro A. H.: 1958, The Dynamics and Thermodynamics of Compressible Fluid Flow, John Wiley and Sons.

[14] Spring P., Piechna J., and Onder C.: 2004, Modeling and validation of a pressure-wave supercharger using a finite difference method IMECE2004-59533.

[15] Weber H. E.: 1995, Shock Wave Engine Design, John Wiley and Sons, New York.

Numeryczne studium pracy falowego, dyskowego mikro-silnika

Streszczenie

W pracy przedstawiono idę, konstrukcję, model numeryczny oraz wyniki numerycznej symulacji pracy mikro-silnika wykorzystującego w zasadzie swojej pracy efekty nieustalonego przepływu gazu. Pokazano pierwsze praktyczne wykorzystanie idei dysków falowych w konstrukcji mikro-silnika falowego. Przedstawiono schemat przepływu powietrza i gazów spalinowych przez ruchome i nieruchome kanały silnika. Pokazano schemat procesów falowych występujących w silniku oraz ich powiązanie z parametrami stanu (ciśnieniami i prędkościami) na płaszczyźnie stanu. Przedstawiono wyniki numerycznej symulacji pracy silnika w postaci rozkładów ciśnienia, prędkości i temperatur w poszczególnych obszarach przepływu w mikro-silniku. Przedstawiono obszar potencjalnych zmian parametrów pracy silnika (strumienia ciepła i prędkości obrotowych dysku) określających stabilną pracę silnika. Oszacowano sprawność silnika o omawianej konstrukcji.